JOURNAL OF NEUROTRAUMA
Volume 21, Number 6, 2004
© Mary Ann Liebert, Inc.
Pp. 000–000

Synthetic Hydrogel Guidance Channels Facilitate Regeneration of Adult Rat Brainstem Motor Axons after Complete Spinal Cord Transection

EVE C. TSAI,[1] PAUL D. DALTON,[2] MOLLY S. SHOICHET,[3] and CHARLES H. TATOR[4]

ABSTRACT

Synthetic guidance channels or tubes have been shown to promote axonal regeneration within the spinal cord from brainstem motor nuclei with the inclusion of agents such as matrices, cells, or growth factors to the tube. We examined the biocompatibility and regenerative capacity of synthetic hydrogel tubular devices that were composed of poly(2-hydroxyethyl methacrylate-co-methyl methacrylate) (PHEMA-MMA). Two PHEMA-MMA channels, having a mean elastic modulus of either 177 or 311 kPa were implanted into T8-transected spinal cords of adult Sprague Dawley rats. The cord stumps were inserted into the channels and fibrin glue was applied to the cord-channel interface. An expanded polytetrafluoroethylene (ePTFE) membrane was used for duraplasty. Controls underwent cord transection alone. Gross and microscopic examination of the spinal cords showed continuity of tissue within the synthetic guidance channels between the cord stumps at 4 weeks. There was a trend towards an increased area and width of bridging neural tissue in the 311-kPa guidance channels compared to the 177-kPa channels. Neurofilament stained axons were visualized within the bridging tissue, and serotonergic axons were found to enter the 311-kPa channel. Retrograde axonal tracing revealed regeneration of axons from reticular, vestibular, and raphe brainstem motor nuclei. For both channels, there was minimal scarring at the channel-cord interface, and less scarring at the channel-dura interface compared to that observed next to the ePTFE. The present study is the first to show that axons from brainstem motor nuclei regenerated in unfilled synthetic hydrogel guidance channels after complete spinal cord transection.

Key words: axonal regeneration; complete spinal cord transection; guidance channel; hydrogel; spinal cord

INTRODUCTION

SPINAL CORD INJURY can be devastating with little or no recovery of function. In adult humans and other mammals, axons of the central nervous system undergo little or abortive regeneration. Within the past twenty years, however, several repair strategies have been devised that allow regeneration of central axons within the

[1]Toronto Western Hospital Research Institute and Krembil Neuroscience Centre, University of Toronto, Toronto Western Research Institute, Toronto Western Hospital, Toronto, Ontario, Canada.

[2]Department of Textile and Macromolecular Chemistry, RWTH-Aachen, Aachen, Germany.

[3]Departments of Chemistry and Chemical Engineering & Applied Chemistry, Institute of Biomaterials and Biomedical Engineering, University of Toronto, Toronto, Ontario, Canada.

[4]Division of Cellular and Molecular Biology, Toronto Western Research Institute, Toronto, Ontario, Canada.

spinal cord. These strategies involve delivery of single or multiple neurotrophic factors (Hiebert et al., 2002; Namiki et al., 2000; Schnell et al., 1994; Tuszynski et al., 1998), neutralization of inhibitory molecules that are believed to inhibit axonal regeneration (Bradbury et al., 2002; Fouad et al., 2001; Huang et al., 1999), and implantation of several types of cells (Coumans et al., 2001; Lu et al., 2002; Ramon-Cueto et al., 1998; Xu et al., 1995) and matrices (Oudega et al., 1997; Teng et al., 2002; Woerly et al., 2001; Xu et al., 1997). While improved axonal regeneration has been reported, recovery after complete spinal cord transection has been minimal. Therefore, a combination of strategies may be required to improve the extent of functional recovery and to achieve a therapeutic approach suitable for application to humans.

With most of the animal studies mentioned above, partial spinal cord injury models were used. While partial spinal cord injury models may more adequately reflect the injuries sustained by man, these models make it difficult to ascertain, whether axons truly regenerated or whether the axons arose as collaterals from intact axons or were axons that were spared from injury. To eliminate this uncertainty, complete spinal cord transection models have been utilized. However, for several reasons, few strategies have produced axonal regeneration and shown functional recovery after complete transection (Cheng et al., 1996; Coumans et al., 2001; Lu et al., 2002; Ramon-Cueto et al., 1998; Rapalino et al., 1998; Schwartz et al., 1999). With complete cord transection, the two spinal cord stumps may retract, thereby eliminating a surface upon which axons can regenerate. The stumps can develop a fibrous or astrocytic scar, which may also prevent axonal regeneration. Furthermore, the lack of a cavity associated with complete transection injuries, makes drug injection, cell implantation, or other reparative strategies difficult, as there is no cavity to contain the inserted material.

To permit examination of a combination of strategies, and to study true axonal regeneration after complete transection of the spinal cord, we and others (Oudega et al., 2001; Spilker et al., 2001; Teng et al., 2002; Xu et al., 1995; Xu et al., 1999) have pursued an entubulation strategy to promote axonal regeneration in the completely transected spinal cord, similar to the strategy used for peripheral nerve repair (Fields et al., 1989; Lundborg et al., 1981; Mackinnon and Dellon, 1990). Entubulation is a technique used for axonal regeneration in the peripheral nervous system (Dahlin and Lundborg, 2001), where the nerve guidance channels, or tubes, are essentially cylindrical structures in which the stumps of a fully transected nerve are placed in either end. Tubes have been shown to both prevent the influx of external cells (Guest et al., 1997) and to concentrate the molecules excreted from the nerve stumps by restricting their diffusion away from the injury area (Aebischer et al., 1988; Rodriguez et al., 1999). The channels can be designed to create a permissive environment for regeneration and can contain a combination of the necessary components for repair such as trophic factors (Bloch et al., 2001), gel matrices (Chamberlain et al., 1998; Wells et al., 1997), cell transplants (Guenard et al., 1992; Verdu et al., 1999), neutralizers of inhibition, and cell-invasive scaffolds (Meek et al., 1996).

Comparable tubular guidance channel strategies have been tested in the central nervous system specifically to promote axonal regeneration of the completely transected spinal cord. These studies include the use of Millipore tubes (Campbell et al., 1957) and polycarbonate film tubes coated with poly-L-lysine (Montgomery et al., 1996). Naturally derived channels manufactured from collagen have also been used either empty or supplemented with phosphate buffered saline, large-pore collagen-glycosaminoglycan (GAG) matrix, or small-pore collagen GAG matrix (Spilker et al., 1997, 2001). Biostable synthetic polymeric channels (i.e., polyacrylonitrile:polyvinylchloride copolymer) and biodegradable polyester channels (i.e., poly[D,L-lactic acid]), both of which have also been supplemented with a matrix and/or cells (Chen et al., 1996; Gautier et al., 1998; Oudega et al., 2001; Xu et al., 1995, 1997, 1999) have also been implanted in the transected rat spinal cord.

To improve upon the axonal regeneration and functional recovery that has been obtained with other channels, we designed a novel synthetic hydrogel channel. The synthetic hydrogel channel was designed to have an elastic modulus similar to that of the spinal cord, which has been estimated between 200 and 600 kPa (Chang et al., 1988; Dalton et al., 2002; Hung et al., 1981) because a mismatch in mechanical properties between the implant and the surrounding tissue can result in implant failure (Salacinski et al., 2001; Taylor et al., 1999) or can cause the channel to compress or lacerate the relatively soft spinal cord tissue. We previously demonstrated that these channels are permeable to small nutrient molecules such as glucose and oxygen (Dalton et al., 2002; Luo et al., 2001), which may be important to axonal regeneration.

The goal of this research was to determine the inherent regenerative capacity of empty or unfilled hydrogel channels—that is, channels initially devoid of any added matrix or cell—in a complete spinal cord transection model in the adult rat. We found our channel formulations to be biocompatible based on minimal scarring and inflammation of spinal cord tissue. Remarkably, we also found that a tissue bridge containing many regenerated axons, some from brainstem neurons, formed within these channels. The regenerated bridge within the chan-

nel was also examined for astrocytes, oligodendrocyte precursors, microglia and macrophages.

MATERIALS AND METHODS

Channel Fabrication

All chemicals for the fabrication of the channels were purchased from Aldrich Chemical Co (Milwaukee, WI) and used as received unless indicated otherwise. Water was distilled and deionized at 18OM. Channels were produced by a new liquid-liquid centrifugal spinning technique previously described in detail (Dalton et al., 2002; Dalton and Shoichet, 2001). Briefly, the monomers, 2-hydroxyethyl methacrylate (HEMA) and methyl methacrylate (MMA), were dissolved in excess water. To this were added aqueous solutions of ammonium persulfate (APS) and sodium metabisulfite (SMBS), which comprised the initiating system. This solution was injected into a 15-cm glass mold that was placed in the chuck of a horizontally mounted stirrer. Rotation commenced at a pre-determined speed, as measured with a tachometer (model 461893; Extech Instruments, Waltham, MA). As the monomer was polymerized, the polymer became insoluble in the aqueous solution and phase separated. This separated phase was denser than water and pushed to the periphery of the glass mold by centrifugal forces. After approximately 5 h, glass molds were removed from the drills and the PHEMA-MMA hydrogel channel removed from the mold. The hydrogel channels were cut into 6-mm lengths and extracted (using a Soxhlet extractor) overnight in water to remove residual or unreacted monomer, initiator or crosslinking agent from the resulting tube. Channels were individually packaged into cryovials with a punctured cap, and sterilized by autoclaving (20 min at 120°C) prior to implantation and characterization. The gross physical properties of the channels were soft and flexible, similar in feel to those of contact lenses.

Electron Microscopy of Channels

Random sterile channels were removed from their packaging and cut laterally. Sections were placed in water-filled eppendorf vials, flash frozen in liquid nitrogen, and then freeze-dried to remove the water by sublimation, thereby maintaining the morphology of the wall structure. Dried cross-sections were mounted on aluminum stubs and conductive paint was applied to ensure conduction of the specimen. After gold-coating, the cross-sections were imaged on a scanning electron microscope (SEM) at 15 kV at a working distance of 15 mm. Representative images of the wall morphology are reported.

Mechanical Testing of Channels

Channels of 25 mm in length were sterilized as previously described and mounted on a micro-mechanical tester (Dynatek Dalta, Scientific Instruments, USA) using barbed fitting and Luer Lok connectors. The hydrogel channels were pulled in tension at a rate of 1%/min, and changes in the load and distance measured. The elastic modulus was calculated from the linear portion of the stress-strain curve and represents the elastic behaviour or rigidity of the channels. Channels that had a mean elastic modulus of 177 ± 26 kPa (mean ± SD; $n = 4$) and 311 ± 57 kPa (mean ± SD; $n = 4$) were implanted and are referred to as 177-kPa channels and 311-kPa channels, respectively. Channels that had a mean elastic modulus of 11 ± 2 kPa were also synthesized, but found to be too weak for handling and implantation.

AU1

Animals and Tracer Materials

Adult, female Sprague Dawley rats (Charles River, St. Constant, Quebec, Canada, 200–500 g) were used for this investigation. Fluoro-Gold (FG) was obtained from Fluorochrome (Denver, CO). The animal protocols were approved by the Animal Care Committee of the Research Institute of the University Health Network in accordance with policies established by the Canadian Council of Animal Care.

Channel Implantation and Functional Assessment

Rats were anesthetized with 2% halothane with 1:2 nitrous oxide to oxygen and then received preoperative cefazolin (40 g) in 5 mL of normal saline subcutaneously. After the T7-9 laminae were removed, the dura was incised in the midline and a synthetic expanded polytetrafluoroethylene membrane (ePTFE; Preclude®, W. L. Gore, Flagstaff, AZ) was sutured to one side of the durotomy with two 8-0 Ethilon sutures. Under an operating microscope the spinal cord at the T8 level and any nearby nerve roots were then transected with microscissors and the transection reinspected under microscopy to ensure complete transection of the spinal cord and all spinal roots in the vicinity. Gelfoam (Pharmacia & Upjohn Inc., Mississauga, Ontario, Canada) was placed in the gap between the two stumps for hemostasis. After removal of the Gelfoam, there was a gap between the two stumps of the spinal cord of approximately 4 mm, and this gap was bridged with the 177-kPa channel in six rats and the 311-kPa channel in 13 rats (Table 1). A small "V" was incised in the dorsal aspect of the channel at the rostral and caudal channel rim prior to implantation. A blunt hook was then inserted under the cut rostral stumps to lift the stump and then lower it through the v-cut of the channel. This was repeated for insertion of the caudal stump into

T1

Table 1. Number of Animals Used per Time Point for Functional (BBB) and Tissue (Histology) Analysis for Control and Guidance Channel Groups

Type of tube implanted	*Survival (weeks)*	*Number of animals analyzed for BBB*	*Number of animals sacrificed for histology*
311 kPa	2	$n = 13$	$n = 2$
	4	$n = 11$	$n = 4$
	8	$n = 7$	$n = 7$
177 kPa	2	Not analyzed	$n = 2$
	4	Not analyzed	$n = 2$
	8	Not analyzed	$n = 2$
Control	8	$n = 9$	$n = 9$

F1

the channel. The stumps were inserted approximately 1 mm into the ends of the channel (Fig. 1). Fibrin glue (20 μL of fibrinogen and 20 μL of thrombin; Aventis Behring, Marburg, Germany) was then applied to the stump-channel interface at both ends. The ePTFE membrane was then positioned such that it covered the channel-cord construct entirely. Control animals ($n = 9$) had the transection at T8, and the synthetic dural membrane was placed between the two stumps and positioned so that one edge of the synthetic dural membrane was ventral to the rostral stump, and the other edge of the membrane was dorsal to the caudal stump. This step was taken to ensure that there would be no tissue continuity established between the two cord stumps.

The wound was closed in layers with 3-0 Vicryl sutures (Johnson & Johnson, Peterborough, Ontario, Canada) in the paraspinal muscles and Michel clips (Fine Science Tools, North Vancouver, B.C., Canada) in the skin. Buprenorphine (0.03 mg/kg, subcutaneously) was given postoperatively and animals had their bladders expressed manually three times a day. Urinary tract infections were treated with ampicillin (125 mg every 12 h, subcutaneously) and gentamicin (2 mg once a day, subcutaneously) was added for urinary tract infections persisting more than 5 days.

Animals with the 311-kPa channels and control animals (Table 1) were assessed weekly for functional behavior with the Basso, Beattie, and Bresnahan (BBB) (Basso et al., 1995) scoring system, and all animals were videotaped while ambulating for 4 min just prior to tracer insertion or perfusion.

Retrograde Axonal Tracing and Immunohistochemistry

The axonal tracer techniques and immunohistochemical techniques were based on techniques that we have previously reported (Tsai et al., 2001). Briefly, rats were anesthetised with 2% halothane with 1:2 nitrous oxide to oxygen. Retrograde tracing with FG was performed in four transection control animals, and in one and four of the animals with 311-kPa channels at 4 and 8 weeks, respectively. After the predetermined period of observation, rats underwent laminectomy at T13 and complete spinal cord transection with microscissors. A pledget of Gelfoam (0.5 mm^2) was soaked in a solution of FG in normal saline (4% for FG) and then placed in the transection site. Petroleum jelly (Sherwood Medical, St. Louis, MO) was then placed over the spinal cord and FG pledget at the laminectomy site, the muscles closed with 3-0 Vicryl and the skin with Michel suture clips. After 7 days, the tissue was prepared as described below and the cord and brain sections examined for evidence of retrograde labeling.

Tissue Preparation

Animals were sacrificed at the end of the planned period of observation or 7 days later if the retrograde tracer was inserted. All animals were sacrificed by intraperitoneal injection of 0.7–1.0 mL of sodium pentobarbital (65 mg/mL). After thoracotomy they received an intracardiac injection of 1 mL of 1000 U/mL heparin, and then the animals that had axonal tracing were perfused with 500 mL of 4% paraformaldehyde in 0.1 M phosphate buffer (PB), and the rest were perfused with 500 mL of 10% neutral buffered formalin.

For the animals with axonal tracers, the brain and spinal cord were removed, cryoprotected with 30% sucrose in PB (24 h, 4°C), and then frozen and embedded in Optimum Cutting Temperature (OCT) compound (Stephens Scientific, Riverdale, NJ). Coronal sections of the entire brain were cut in a cryostat at 40 μm, whereas serial parasagittal sections of a 1.5–2-cm length of spinal

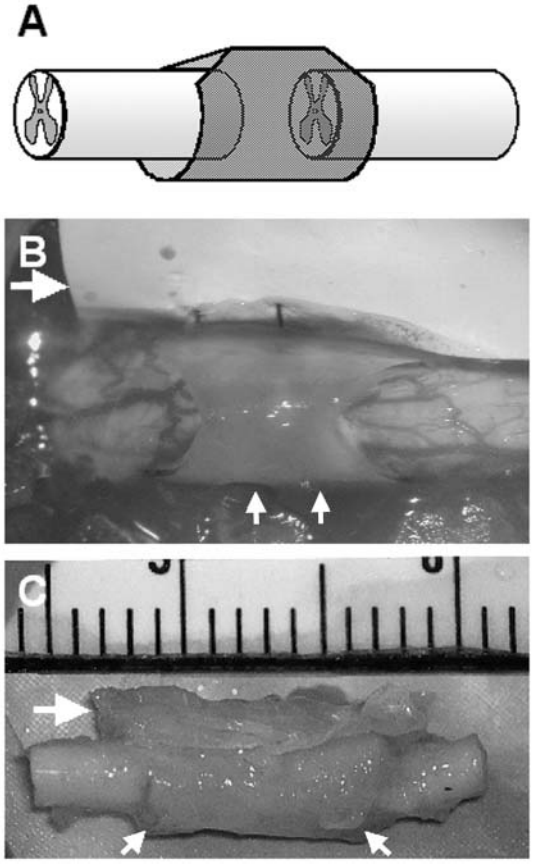

FIG. 1. **(A)** Schematic showing a lateral view of the transected ends of the spinal cord stumps within the channel. **(B)** Intraoperative photograph showing the dorsal aspect of the spinal cord stumps placed within the semitransparent channel. The gap between the cord stumps is indicated by the small white arrows. The ePTFE membrane (large white arrow) is placed over the cord-PHEMA-MMA channel repair site after channel insertion. **(C)** Spinal cord containing the 311-kPa channel implant excised after 4 weeks. Note the junction of the cord stumps and the channel delineated by the small white arrows. The ePTFE membrane (large white arrow) is also visualized. Ruler markings are in millimeters.

cord encompassing the transection site (Fig. 1C) and the transplanted channel were cut at 20 μm in a 1:6 series and mounted on cold (−20°C) Superfrosted Plus slides (Fisher Scientific, Markham, Ontario, Canada). To investigate the presence of labeled propriospinal neurons, six serial transverse spinal cord sections (20 μm thick) were taken at the T3, T4, and T5 spinal cord levels.

It has been observed that animals with neurological disease (Dowson and Harris, 1981; Stojanovic et al., 1994), and specifically spinal cord transection (Tsai et al., 2001), show significant autofluorescence of cortical, brainstem and spinal neurons that may interfere with identification of FG labeling. To eliminate this autofluorescence artifact, the brain and transverse spinal cord sections were left to dry and treated for autofluorescence as described previously (Tsai et al., 2001) prior to the examination for FG labeled neurons. Briefly, three techniques, the Sudan Black B technique, the cupric sulfate technique, and the multiple filter block technique were used to differentiate autofluorescent cells from FG labeled cells. Both the Sudan Black B and the cupric sulfate decrease the signal from autofluorescent cells only, and do not eliminate the signal from immunolabeled or FG labeled cells. For the parasagittal spinal cord sections, the Sudan Black B technique was used. These sections on slides were dipped in Tris buffer (TB; Fisher Scientific, Markham, ON, Canada; pH 8.0) and then 70% ethanol. Sections were then stained with 0.3% SBB (BDH, Toronto, ON, Canada) in 70% ethanol for 10 min, and washed in TB.

The cupric sulfate technique was used for the brain sections and transverse spinal cord sections. These sections on slides were washed with 0.1 M phosphate buffered saline (PBS), dipped in distilled water, and treated with 0.5% $CuSO_4$ (Sigma, St. Louis, MO) in ammonium acetate buffer (50 mM, pH 5.0; Sigma) for 10 minutes, washed with 0.1 M PBS, and then visualized hydrated. Sections that dried prior to viewing were rehydrated with PBS.

All sections were then further examined with the multiple filter block technique where neurons were examined with three different filter blocks as described below. A structure was considered labeled only if the fluorescent signal appeared with the appropriate filter block and did not appear with the other filter blocks. For example, a neuron was considered labeled with FG if it fluoresced with only the UV-2A filter block. With the FG neuron counts, the possibility of counting the same cell twice was eliminated by counting every second section. Spinal cord sections were examined for FG using a fluorescent microscope and filter blocks as described below. Paraformaldehyde-fixed sections for immunohistochemistry were kept hydrated with PBS.

For the formalin-fixed animals, a 1.5–2-cm length of spinal cord that encompassed the transection site and channel was removed, photographed, and embedded in paraffin. Serial parasagittal sections 8 μm thick were cut in a 1:8 series, and every eighth section was stained with Luxol Fast Blue with hematoxylin and eosin to determine the series that had a tissue bridge that was the widest and that had the greatest area. All sections of that series then underwent staining with Masson's trichrome, Von Kossa silver stain or Alizarin red S stain for calcium, Prussian blue for iron, or immunohistochemistry for NF200, GFAP, ED1, and NG2 as described below.

Immunohistochemistry

The spinal cord repair site was examined for immunohistochemistry with the following monoclonal antibodies: mouse anti-neurofilament 200, phosphorylated and non-phosphorylated clone N52 (NF200; 1:500, Sigma [Schumacher et al., 1999]) to visualize neurons and axons; mouse anti-glial fibrillary acidic protein (GFAP; 1:200, Boehringer-Mannheim Chemicon, Temecula, CA [Agrawal et al., 1998]) to visualize astrocytes and astrocytic scarring; mouse anti-rat monocytes/macrophages (ED1; 1:200, Chemicon [Fitch et al., 1999; Popovich et al., 1997]) to visualize activated macrophages or microglia. Polyclonal antibodies included: rabbit anti-calcitonin gene related peptide (CGRP; 1:3000, DiaSorin, Stillwater, MN [Brook et al., 1998]) to identify sensory axons; rabbit anti-serotonin (5-HT; 1:10 000, DiaSorin, Stillwater, MN [Brook et al., 1998]) to identify serotonergic axons; and rabbit anti-NG2 chondroitin sulfate proteoglycan (NG2; 1:800, Chemicon, Temecula, CA [Levine and Nishiyama, 1996]) to identify oligodendrocyte precursor cells. In all of the immunohistochemistry procedures appropriate negative controls were made with the omission of the primary antibodies.

Immunohistochemistry of Paraformaldehyde-Fixed Tissue

Every sixth section of the spinal cord repair site of the paraformaldehyde perfused animals was examined using the UV2A filter to select the series that had a tissue bridge that was the widest and that had the greatest area. All sections of that series then underwent immunohistochemistry. The sections were washed three times with PBS for 10 min, and then blocked for endogenous peroxidase and/or then for nonspecific antibody binding. Endogenous peroxidases were blocked with 1% hydrogen peroxide for 30 min for GFAP and NG2 labeling, and for 10 min for 5HT and CGRP. Nonspecific antibody binding was blocked at room temperature (RT) for 1 h with the following: 10% heat-inactivated goat serum (HIGS) in PBS containing 0.3% Triton X-100 for NF200 and GFAP; 20% HIGS in PBS for NG2, 4% normal goat serum (NGS) in PBS containing 0.1% Triton X-100 for ED-1. The primary antibodies were then applied to the sections and incubated overnight at 4°C. All primary antibodies were diluted in blocking solutions with the exception of the following: 5-HT and CGRP were diluted in 0.3% Triton X-100 in PBS; and NG2 was diluted in PBS. Sections were then washed three times in PBS, and incubated with the secondary antibody, Alexa Fluor™ 488 goat anti-mouse and goat anti-rabbit IgG (H+L) conjugate highly cross-adsorbed (1:500 dilution in PBS; Molecular Probes, Eugene, OR), was applied for 1 h at RT. Sections were mounted without coverslipping and viewed hydrated with PBS using a fluorescent microscope as described below.

Immunohistochemistry of Formalin-Fixed Tissue

Formalin fixed sections were deparaffinized and slides for ED-1 were postfixed in Bouin's for 1 h at 60°C. All sections were blocked for endogenous peroxidase with 1% methanol peroxidase for 30 min, except for those stained for NF200, and GFAP. To unmask antigen sites, selected sections of slides for ED-1 and NG2 were placed in a pressure cooker with citrate buffer (pH 6.0) and heated in a microwave oven (Kenmore Sears Canada Inc., model 88952) for 35 min on high. After heating, slides remained in the microwave for an additional 30 min and were then rinsed with PBS twice. For NF200, a solution of ethylenediaminotetraacetic acid (EDTA) in pH 8 buffer was heated in the microwave for 15 min on high power. The slides were then placed in the EDTA solution in the pressure cooker, which was placed in the microwave for 8 min on high power. After heating, the slides were left in the microwave for 20 min and then rinsed with PBS twice. All sections were blocked for nonspecific antibody binding as previously described. Monoclonal antibodies ED-1 (1:50, Chemicon), GFAP (1:200, Chemicon), NF 200 (1:400, Sigma), and the polyclonal antibody NG2 (1:250, Chemicon) were then applied and incubated overnight at 4°C. The primary antibodies were diluted in blocking solutions, with the exception of NG2 which was diluted in PBS, the appropriate biotinylated secondary antibodies and avidin-biotin peroxidase complex (Vectostain Elite ABC Kit Standard, Vector Laboratories, Burlington, Ontario, Canada) were then added. Vector VIP (VIP, Vector Laboratories) was applied as the chromogen. Sections were coverslipped with Entellan (EM Science, Gibbstwon, NJ) and visualized under a light microscope (Nikon Eclipse TE300, Nikon Mississauga, Ontario, Canada).

Visualization of Retrograde Axonal Tracing and Fluorescent Immunohistochemistry

A fluorescent microscope (Nikon Eclipse TE300) was used for fluorescence histological examination with the following filter blocks: Tx Red (excitation filter 540–580 nm, dichroic mirror DM 595, barrier filter BA600–660); G-2A (excitation filter 510–560, dichroic mirror DM575, barrier filter BA590); B-2E (excitation filter 450–490, dichroic mirror DM 505, emission 520–560); and UV-2A (excitation filter 330–380, dichroic mirror DM 400, barrier filter BA420). Images were captured with an Op-

tronics digital camera and the Bioquant Nova Prime for Windows 9x Version 6.50.10 MR.

Measurement of Bridging Tissue Area, Bridging Tissue Widths, and Stump Gap Lengths

All paraffin sections were examined from all animals to determine the size of the tissue bridging between the stumps within the channel. Three serial parasagittal sections containing the largest tissue bridge were selected and measured for bridging tissue area, bridging tissue widths, and stump gap lengths using Bioquant Imaging Software. Total bridging tissue area was measured by outlining the bridging tissue within the channel and limited by the GFAP scar at the rostral and caudal ends. The width of the bridging tissue was measured at the point where the bridging tissue was the widest. Stump gap length was defined as the shortest distance within the channel between the two cord stumps with the GFAP labeled scar delimiting the rostral and caudal ends of the cord stumps. For measurement of the stump gap length, only animals that had a tissue bridge were included in the analysis.

Measurement of ED1 Density

For measurement of ED1 density, four formalin fixed parasagittal sections from transection control animals ($n = 3$) and from animals with 311-kPa channels ($n = 3$) implanted for 8 weeks were stained for ED1 and examined. Using a standardized scan area or rectangular region of interest, the entire dorsoventral aspect of the cord through the stumps and through the tissue bridge was measured using Bioquant to obtain the measurement of the area of ED1 staining. Scan areas that did not include tissue were subtracted from the area encompassed from the region of interest rectangles. Density was calculated by dividing the area of ED1 staining by the area encompassed by the region of interest rectangles. For all sections, the same light and threshold levels were maintained.

Statistics

BBB scores were analyzed with two-way repeated measures ANOVA and post-hoc analysis was performed using the Bonferroni method. Comparison of the number of brainstem motor nuclei neurons labeled with FG and ED1 labeling in control and 311-kPa implanted animals was performed with one way analysis of variance. Analysis was performed with SigmaStat for Windows Version 2.03 and Microsoft® Excel 2000, and graphs were drawn with SigmaPlot for Windows Version 4.01.

RESULTS

Hydrogel Spinal Cord Channels

Hydrogel guidance channels were designed to match the dimensions and modulus of the rat spinal cord. The outside diameter of the channels was approximately 4.2 mm, and the inside diameter was 3.6 mm, giving a wall thickness of 0.3 mm. All channels were flexible, soft to touch and had similar dimensions. Concentric hydrogel guidance channels were produced with different elastic moduli and wall morphologies (Fig. 2). Spinal cord channels had an elastic modulus of 11 ± 2, 177 ± 26, and 311 ± 57 kPa (mean $\pm$ SD). The 11-kPa channels collapsed easily, which made handling and implantation difficult. The 177-kPa and 311-kPa channels were easier to handle and implant. As shown in Figure 2 with SEM images, the 177-kPa channel had a "spongy" porous wall morphology, while the 311-kPa channel had a predominately gel-like morphology.

F2

Tissue Bridge Between Cord Stumps—Minimal Fibroblastic or Glial Scarring

Hydrogel channels were implanted in spinal cord transected adult rats for 2–8 weeks and assessed for their ability to serve as a pathway for regeneration. At 2 weeks, no tissue bridge was evident in either the 177-kPa or the 311-kPa spinal cord channels. However, at 4–8 weeks, a tissue bridge was evident in both channels. There was a tissue bridge at 4 weeks or later in the majority of animals implanted with the 177-kPa channels ($n = 3$ of 4) and the 311-kPa channels ($n = 10$ of 11) (Fig. 3). For the 177-kPa channels, a tissue bridge was present in one of two animals at 4 weeks and two of two animals at 8 weeks. For the 311-kPa channels, a tissue bridge was present in four of four animals at 4 weeks and six of seven animals at 8 weeks.

F3

The mean total bridging area for the 311-kPa and the 177-kPa channels was $621 \times 10^4 \pm 98 \times 10^4$ μm^2 and $68 \times 10^4 \pm 36 \times 10^4$ μm^2 (mean $\pm$ SEM), respectively. The mean width of the tissue bridge was 793 ± 100 μm for the 311-kPa tubes compared to 91.8 ± 41.8 μm for the 177-kPa tubes. Although the small number of animals that received the 177-kPa channel precludes meaningful statistical analysis, there appeared to be a trend toward a larger tissue bridge in the animals that received the 311- versus the 177-kPa channel.

The Masson stain revealed no difference in the extent of fibroblastic reaction and collagen formation between the two types of guidance channels. For both there was minimal fibroblast infiltration/collagen deposition in the lumen of the guidance channel compared to the amount of scarring outside of the guidance channel next to the

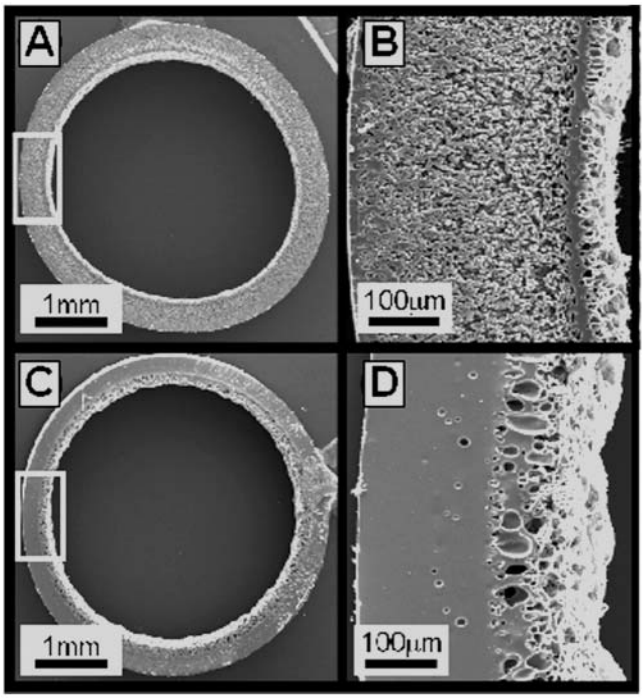

FIG. 2. Scanning electron micrographs of hydrogel channels. Cross-sections of a 177-kPa channel **(A)** and increased magnification revealing the wall morphology **(B)**, and a 311-kPa channel **(C)** and increased magnification of the wall structure **(D)**.

ePTFE membrane. While there was some scar/collagen deposition adjacent to the synthetic ePTFE dural membrane, there was remarkably less collagen within the tissue bridge and at the interfaces between the spinal cord stumps and the tissue bridge, the spinal cord stumps and the guidance channel, and the tissue bridge and the guidance channel (Fig. 4).

F4

There was a dense accumulation of astrocytes as shown by GFAP labeling in both the rostral and caudal stumps of the transected cord, as has been reported in other channel implantation studies (Chen et al., 1996; Oudega et al., 1997). Astrocytes did not appear to migrate into the middle of the tissue bridge. GFAP labeling has been used to define the border between spinal cord stump and the tissue graft or bridge (Guest et al., 1997). The distance between the spinal cord stumps, as defined by GFAP labeling see (Fig. 5), for the 311 kPa and 177 kPa channels was 6.42 ± 0.84 mm and 7.16 ± 0.32 mm, respectively. The similar spinal cord stump distance of both the 177 and the 311 kPa groups suggests that the increase in the size of the tissue bridge in the 311 kPa group is due to the increased growth of new tissue rather than decreased atrophy of the transected spinal cord stumps in the 311 kPa channel group.

F5

As there was a trend for an increased area and width of the tissue bridge in the 311-kPa channels, only rats implanted with these channels and controls were then further characterized for histology and behaviour.

Neural Tissue

Numerous axons were present in the tissue bridge that formed within the channels as demonstrated with NF200 staining. Axons seemed to be more abundant in the bridging tissue near the channel walls (Fig. 6) suggesting that the inner channel wall surface may support elongation of regenerating axons and may promote the alignment of the regenerating axons. This location also corresponded to areas of greatest myelination as seen with hematoxylin and eosin/Luxol Fast Blue staining of adjacent sections (Fig. 7).

F6

F7

In an attempt to identify the different types of axons growing within the newly formed tissue bridge, we used multiple stains. Although serotonergic 5HT supraspinal axonal fibers were found to extend from the rostral stump into the channel, only one animal had a small number of 5HT fibers in the caudal stump. Axons of dorsal root origin stained with CGRP, were also present in the bridging tissue. However, the number of fibers that stained positively for 5HT or CGRP did not account for all of the fibres that stained positively for NF200, suggesting that other types of axons regenerated into the channels (Fig. 3).

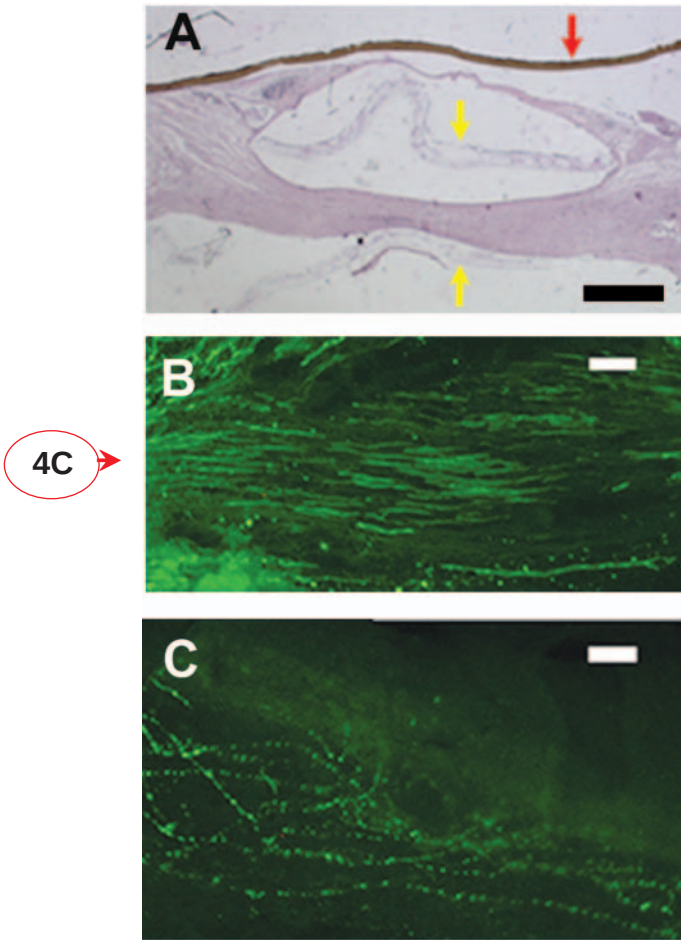

FIG. 3. PHEMA-MMA channels facilitate tissue and axonal regeneration. **(A)** Hematoxylin and eosin–stained section showing tissue that regenerated within the channel walls (yellow arrows). The ePTFE membrane (red arrow) is seen dorsal to the channel. Note the thick tissue bridge that has regenerated after complete cord transection (bar = 1 mm). A parasagittal section through the tissue bridge of an animal that received a 311-kPa channel for 8 weeks stained for NF200 to label axons **(B)** and CGRP to label sensory axons **(C)**. Note the many regenerating axons, labeled green, within the tissue bridge. The number of fibers that stained positively for CGRP did not account for all of the fibres that stained positively for NF200, suggesting that other types of axons regenerated into the channels (bar = 10 μm).

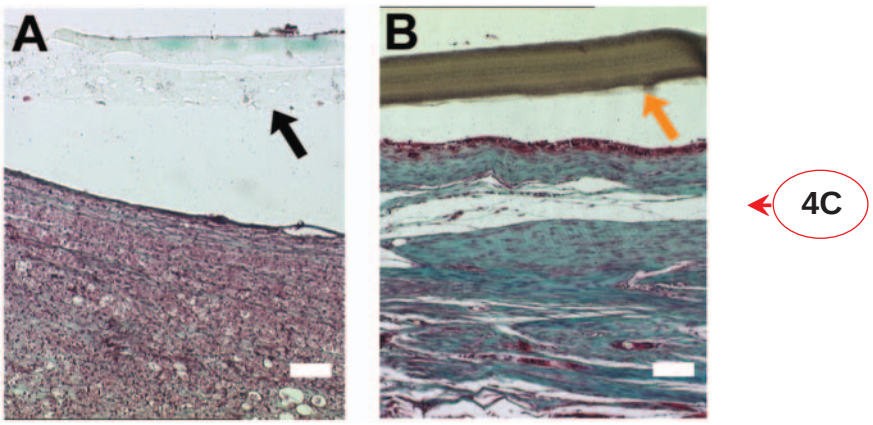

FIG. 4. Histological sections from the spinal cord repair site 4 weeks post-implantation of a 311-kPa PHEMA-MMA channel. Section is stained with Masson's trichrome for collagen (collagen stains green). Note the minimal deposition of collagen scar next to the 311-kPa PHEMA-MMA channel (**A,** black arrow) compared to the thick collagen deposition adjacent to the expanded polytetrafluoroethylene membrane (**B,** orange arrow; bar = 100 μm). During processing of the tissue, the guidance channel walls often separated from adjacent tissues because there was increased shrinkage of the tissue compared to the channel. Therefore, histological preparations often show guidance channel buckling or separation (Fig. 3), which was not apparent before formalin fixation and paraffin processing.

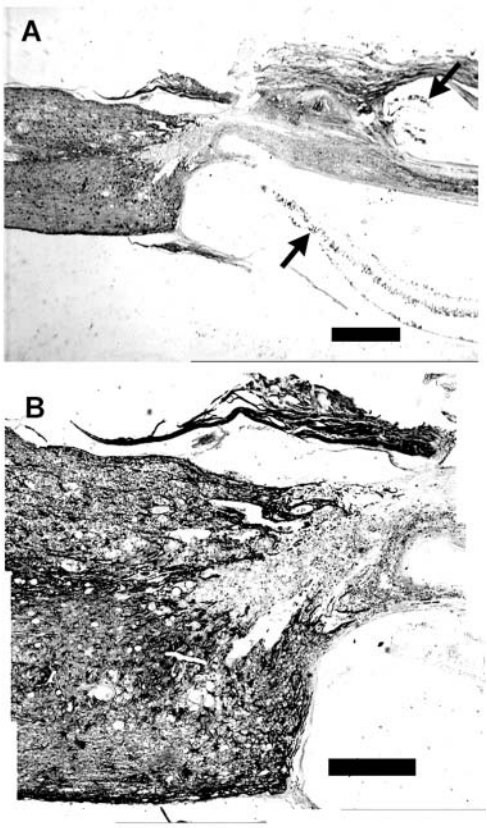

FIG. 5. Astrocyte accumulation at the interface between the stump and bridging tissue. A parasagittal section of the spinal cord **(A)** stained for GFAP from an animal that had received a 311-kPa channel for 8 weeks. The rostral stump is to the left and the bridging tissue is on the right of the figure. Dorsal is to the top of the figure. Due to tissue processing, the guidance channel, which is indicated by the arrows, has been displaced from its *in vivo* position adjacent to the tissue bridge. Note that there is dense GFAP labeling of the rostral stump and relatively little GFAP present within the tissue bridge (bar = 1 mm). **(B)** A photomicrograph montage showing a higher power view of the rostral stump—tissue bridge interface. Note the distinct margin between the cord and tissue bridge. Bar = 500 μm.

Axonal Tracers

To further characterize the origin of axons that regenerated into the 311-kPa channels, retrograde axonal tracing with FG was performed in four of the 8-week survival animals. Motor nuclei of controls and propriospinal neurons of both control and repair groups were examined and found to contain no FG labeled neurons. The lack of FG labeling in these locations corroborates that the motor nuclei FG labeling observed in repair animals was not due to diffusion of FG, as FG labeling of the neurons in these locations would occur if there was diffusion of the FG tracer. The lack of labeling of the propriospinal neurons in both repair and control animals indicate that the channel alone does not promote regeneration of propriospinal axons.

In the animals of the repair group, however, neurons in the reticular, vestibular and raphe nucleus were found to be retrogradely labeled with FG (Fig. 8) by axons that had regenerated through the guidance channels to the T13/L1 level, a distance of approximately 2.5 cm from the transection site. The mean neuronal counts of labeled FG neurons in the reticulospinal, vestibulospinal, and raphespinal nuclei were 10.3 ± 6.4, 12.3 ± 6.9, and 2.7 ± 2.7 (mean $\pm$ SEM), respectively. Many of the brainstem neurons showed major morphological changes, likely related to the complete axonal transection injury which is known to modify neuronal cell bodies (Kwon et al., 2002; Liu et al., 2002).

All sections were examined with both the cupric sulphate and multiple filter techniques to ensure that autofluorescent cells were eliminated from the counts. The use of both these techniques will also eliminate cells that are both autofluorescent and FG labeled, and thus the counts listed above may underestimate the true extent of neurons that regenerated axons. Although the counts may have been underestimated, there was nevertheless more brainstem motor neurons labeled with FG found in the repair animals compared to controls (one way analysis of variance, Dunnett's method for multiple comparisons versus control group, $p = 0.002$). The specific nuclei that showed regeneration include the dorsal reticular medullary nucleus and the lateral reticular nucleus, the lateral, median, and superior vestibular nuclei, and the raphe obscurus nucleus.

Myelinating Cell Precursors within the Tissue Bridge

NG2-labeled cells, which could be oligodendrocyte precursors cells (Ong and Levine, 1999; Watanabe et al., 2002) or Schwann cells (McTigue et al., 2001), were also found within the cord stumps and tissue bridge. The NG2 cells of the stumps, however, were stellate and located predominately within the grey matter. In contrast, the NG2 labeled cells within the bridging tissue were elongated and aligned along the rostral-caudal axis in a similar direction and location to the regenerating axons (Fig. 9). This suggests that NG2 cells may have migrated into the channel and may be myelinating or guiding the regenerating axons.

Inflammation and Scarring

Macrophages and microglia were found throughout the cord stumps, more in the white matter compared to the

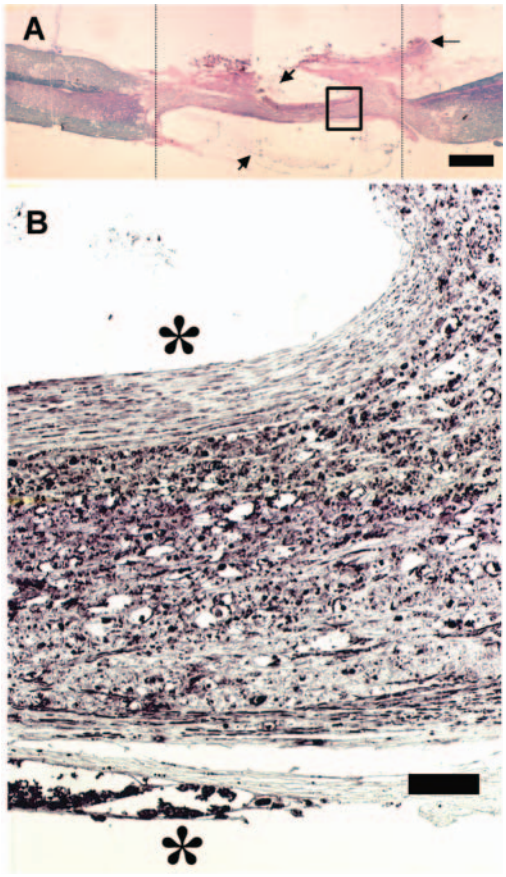

4C

FIG. 6. Axons are present in the bridging tissue eight weeks after complete spinal cord transection and repair with a 311-kPa channel. A parasagittal section of the spinal cord **(A)** at the repair site stained with Luxol Fast Blue and hematoxylin and eosin. The bridging tissue lies between the two hatched lines. Note the myelinated white matter tracts are predominately blue in colour. Rostral is to the left and dorsal is to the top of the figure. Bar = 1 mm. Short arrows indicate the channel, and the longer arrow indicates scar tissue overlying the channel. **(B)** A higher power view of the boxed area in A, showing an adjacent parasagittal section stained for axons (NF200). The asterisks denote the location of the channel wall. Note the numerous linear axons adjacent to the channel walls. Bar = 100 μm.

grey matter, as well as within the tissue bridge. The density of ED1 labeled cells (mean ± SD) was $132 \times 10^{-3} \pm 64 \times 10^{-3}$ μm^2 within the tissue bridge and $154 \times 10^{-3} \pm 46 \times 10^{-3}$ μm^2 within the white matter. There was no significant difference (one way analysis of variance, $p = 0.325$) in the distribution of the macrophages within the bridging tissue and the white matter of the cord stumps, indicating that the channel did not increase the inflammatory cell population. The density of macrophages in the stumps of the transection controls was $123 \times 10^{-3} \pm 49 \times 10^{-3}$ μm^2 and in the repair animals was $108 \times 10^{-3} \pm 27 \times 10^{-3}$ μm^2 (mean ± SD). There was no statistical difference (t-test, $p = 0.101$) in the density of macrophages in the stumps between the transection controls and repair animals, also suggesting that the tube did not increase inflammation in the cord.

NF200 positive material was found within macrophages/microglia both within the channel (Fig. 7A) and in the cord stumps. The macrophages/microglia within the cord stumps are likely ingesting either regenerating or degenerating tissue, while those within the bridging tissue may be ingesting regenerating axons. Indeed, in the LFB H&E stained sections, myelin debris was also found within the macrophages/microglia in the tissue bridge, suggesting that macrophages/microglia may also be ingesting newly formed myelin (Fig. 7B).

The Masson stain revealed no difference in the extent of fibroblastic reaction and collagen formation between the two types of guidance channels. For both there was minimal fibroblast infiltration/collagen deposition in the lumen of the guidance channel compared to the amount of scarring outside of the guidance channel next to the ePTFE membrane. While there was some scar/collagen

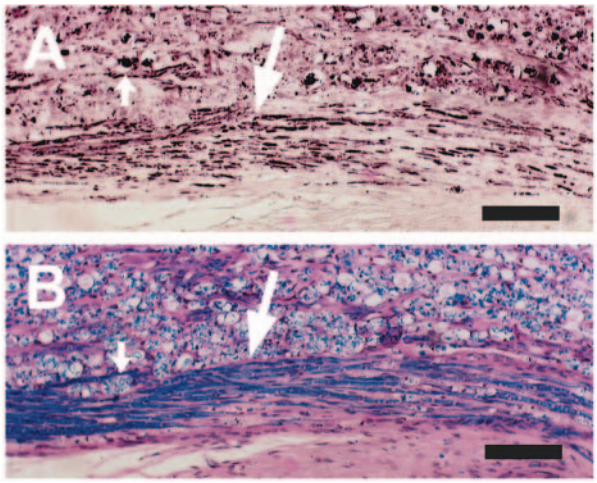

4C

FIG. 7. Regenerated axons are myelinated. Serial parasagittal sections of the same region of the tissue bridge stained with NF200 **(A)** and Luxol Fast Blue **(B)** with hematoxylin and eosin in an animal with an implanted 311-kPa channel for 8 weeks. Note the region of myelin formation (arrow, myelin stains blue) corresponds to the same region containing numerous axons in the tissue bridge, indicating that the newly regenerated axons are myelinated. Small white arrow in A indicates NF200 positive globular material that likely represents a macrophage/microglia cell that has ingested axonal material. The small white arrow in B indicates a macrophage/microglia cell that contains myelin debris, suggesting that macrophages/microglia may also be ingesting newly formed myelin. Bar = 100 μm.

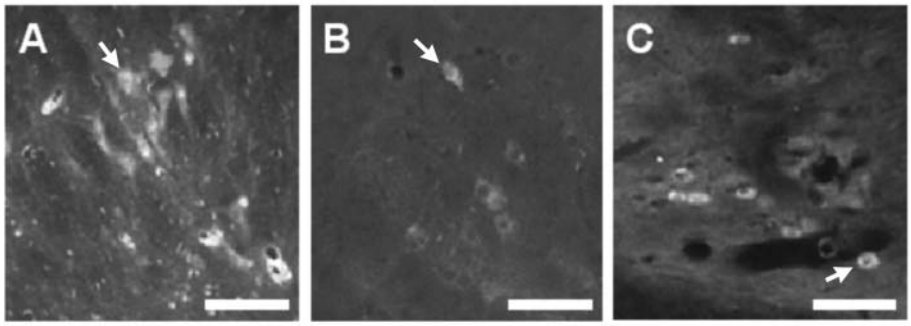

FIG. 8. Retrograde tracing with Fluoro-Gold revealed that neurons (arrows) from several brainstem motor nuclei had regenerated axons through the 311-kPa channel. Motor nuclei with evidence of axonal regeneration included reticulospinal **(A)**, vestibulospinal **(B)**, and raphespinal axons **(C)**. Bar = 20 μm. No FG labeled neurons were found in controls.

deposition adjacent to the synthetic ePTFE dural membrane, there was remarkably less collagen within the tissue bridge and at the interfaces between the spinal cord stumps and the tissue bridge, the spinal cord stumps and the guidance channel, and the tissue bridge and the guidance channel (Fig. 9).

There was a dense accumulation of astrocytes as shown by GFAP labeling in both the rostral and caudal stumps of the transected cord, as has been reported in other channel implantation studies (Chen et al., 1996; Oudega et al., 1997). Astrocytes did not appear to migrate into the middle of the tissue bridge.

Mineral Deposition on the Channels

As early as 2 weeks, calcium was evident on the exterior surface of the channel as demonstrated by the von Kossa and Alizarin red S stain for calcium. At 4 and 8 weeks, there was progressively more calcium deposition on the exterior of the channel. Interestingly, there was minimal calcium deposition on the interior surface of the channel likely because the internal channel environment differed from the external environment. Staining with Prussian Blue revealed minimal deposition of hemosiderin on the channels.

Functional Results

With the BBB scoring system, we assessed locomotor functional recovery in the group with 311 kPa channels and transection controls. There was no significant difference between the groups (Two Way Repeated Measures ANOVA—Bonferroni t-test; $P = 0.128$). The BBB score (mean $\pm$ SD) achieved at 8 weeks for the control and 311 kPa channel group was 1.2 ± 1.0 and 2.3 ± 2.2, respectively.

DISCUSSION

Axons from brainstem motor nuclei regenerated through the synthetic hydrogel channels and bridged a 4

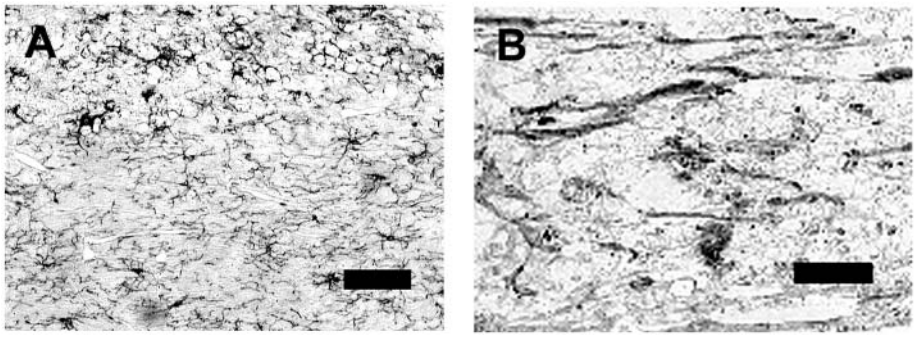

FIG. 9. NG2 labeled cells within the cord stumps **(A)** and the tissue bridge **(B)**. Note how the NG2 cells of the stumps are stellate whereas the NG2 cells of the tissue bridge are elongated. Rostral is to the left, and caudal is to the right. Bar = 100 μm. These cells may have migrated into the channel to myelinate or guide regenerating axons.

mm gap between the stumps of the transected spinal cord of an adult rat. Some of the axons were from motor nuclei and regenerated through the complete spinal cord transection at T8 to at least the T13/L1 cord level, the site of implantation of the FG tracer. While previous studies have demonstrated axonal regeneration within synthetic channels, the present study is remarkable because it is the first to show that axons from brainstem motor nuclei regenerated in unfilled synthetic hydrogel guidance channels after complete spinal cord transection. Our study is unique in that the hydrogel channels were not pre-filled with matrix or cells, and animals were not treated with adjuvant drugs or neurotrophic factors to obtain axonal regeneration from brainstem motor neurons.

In other entubulation studies using a complete transection model (Gautier et al., 1998; Montgomery et al., 1996; Spilker et al., 1997; Spilker et al., 2001) there was no evidence of regeneration of axons from brainstem nuclei through the channel except when channels were augmented with one of the following combination therapies, in which case regeneration of supraspinal axons was observed: (1) guidance channels filled with Schwann cells, Matrigel and methylprednisolone (Oudega et al., 2001); or (2) guidance channels filled with Schwann cells and Matrigel with delivery of neurotrophic factors (Xu et al., 1995; Xu et al., 1999). In our study, regeneration of brainstem axons occurred in animals that were not treated with a growth factor or methylprednisolone, and our channels did not contain cells and were not filled with a matrix. While we acknowledge that some of the fibrin sealant may have leaked into the channel, the amount, if any, would have been inconsequential as fibrin glue solidifies quickly when used as a sealant at the tissue-tube interface. Furthermore, since the channel is translucent, we were able to observe by observation, that the channel was not completely filled with fibrin glue.

It is important to differentiate the complete transection model from the hemi-transection model, where axonal regeneration has also been demonstrated in empty channels (Montgomery et al., 1996). In one hemi-transection study (Xu et al., 1999), Matrigel-filled channels were used to promote propriospinal axonal regeneration. The lack of propriospinal regeneration in our study may be due to the following reasons. In studies in which propriospinal neurons regenerated within channels (Chen et al., 1996; Guest et al., 1997; Oudega et al., 1997; Xu et al., 1997; Xu et al., 1995), Matrigel was used to fill the channel. In preliminary results with Matrigel within our channel (results not published), we found that Matrigel prevented the regeneration of any brainstem motor neurons. Thus, perhaps one reason why propriospinal axons have been perceived to regenerate more vigorously is not a characteristic of propriospinal neurons itself, but because of the matrix through which they are allowed to grow. In other studies that have used collagen to fill the channel, propriospinal neurons did not regenerate more vigorously (Spilker et al., 1997; Spilker et al., 2001).

Another difference between these studies and ours is the choice of axonal tracer. In several studies, Fast Blue was used as the axonal tracer and was injected into the center of the guidance channel (Chen et al., 1996; Xu et al., 1997; Xu et al., 1995). Thus, the Fast Blue may have labeled axons that regenerated into, but not through, the entire length of the tube. Fast Blue is known to label axons with application to the epineurium (Choi et al., 2002) whereas FG is less likely to label fibers of passage (Schmued and Fallon, 1986). The increased likelihood of Fast Blue to label fibers of passage may explain why propriospinal neurons may appear to have regenerated more vigorously in these other studies.

When these Matrigel-filled channels were augmented with Schwann cells, significant brainstem labeling was observed. While these results are important, the hemitransection model is a partial injury model that does not differentiate between re-growth of the transected axons (true axonal regeneration) and axonal growth from non-transected fibres (collateral sprouting). The ideal repair would facilitate regeneration of transected axons (true regeneration) rather than have spared axons replace the transected axons (axonal collateralization).

Achieving true regeneration is not new but the fact that this was achieved with brainstem motor nuclei in simple unfilled channels after complete cord transection is promising and suggests that combination therapies that we test in the future may yield results superior to those published to date. It is unclear why these hydrogel channels are superior to others tested to date; however we speculate that the mechanical properties of the channel, which are similar to those of the spinal cord (Dalton et al., 2002), may be important to maximize tissue regeneration and minimize necrotic tissue at the stump-tissue bridge interface. The permeability of our channel to small nutrient molecules such as glucose and oxygen (Dalton et al., 2002; Luo et al., 2001), may also play a role in improving axonal regeneration. In addition, there may be other unique features of our channel that are as yet unidentified. The overall bioacceptability of the implant material, as evidenced by a minimal inflammatory response, also likely plays an important role for tissue regeneration.

Despite the regeneration of axons from brainstem motor nuclei, functional recovery remains elusive. The potential for greater recovery with the incorporation of combination therapies into these already permissive channels is great. Indeed, these channels permit the addition of a variety of factors to augment axonal regeneration of spe-

cific motor or sensory nuclei, including matrices, growth factors, inhibitory factor neutralizers, and cellular transplants. During fabrication, the PHEMA-MMA channel requires neither high temperatures for molding nor the use of potentially toxic solvents (Friedman et al., 2002), and thus facilitates the incorporation of bioactive compounds such as neurotrophic factors (Bamber et al., 2001; Hiebert et al., 2002; Namiki et al., 2000; Schnell et al., 1994; Tuszynski et al., 1998), enzymes such as chondroitinase ABC (Zuo et al., 1998), antibodies such as IN-1 to neutralize inhibition of axonal regeneration (Fouad et al., 2001; Huang et al., 1999) or cells (Bunge, 1994; Oudega et al., 2001; Xu et al., 1997; Xu et al., 1995). Scaffolds, with a microarchitecture engineered for optimal axon growth and organization, can also be designed to be placed within the channel (Teng et al., 2002).

Although entubulation has been used extensively in peripheral nerve regeneration both experimentally and clinically, entubulation of the spinal cord has received less interest. Our results suggest that synthetic hydrogel channels may hold promise as a novel therapeutic strategy for the treatment of spinal cord injury. The entubulation strategy with synthetic hydrogel channels is advantageous because the channels limit the ingrowth of scar tissue, contain endogenously secreted neurite growth-promoting factors (Oudega et al., 2001), and maintain optimal alignment of both the cord stumps and cells within a tissue cable (Guest et al., 1997). The cure for spinal cord injury will likely require a combination of multiple strategies. The soft, synthetic hydrogel guidance channels that we have described permit the combination of multiple strategies within a controlled spinal cord environment for enhancing true axonal regeneration and, ultimately, functional recovery.

ACKNOWLEDGMENTS

We are grateful to Rita van Bendegem, Kara Marshall, Andrew Grant, and Naana Jumah for their technical assistance. This work was funded in part by the Whitaker Foundation, the Natural Sciences and Engineering Research Council of Canada, the Ontario Neurotrauma Foundation, and the Canadian Institutes of Health Research.

REFERENCES

AEBISCHER, P., GUENARD, V., WINN, S.R., et al. (1988). Blind-ended semipermeable guidance channels support peripheral nerve regeneration in the absence of a distal nerve stump. Brain Res. **454,** 179–187.

AGRAWAL, S.K., THERIAULT, E., and FEHLINGS, M.G. (1998). Role of group I metabotropic glutamate receptors in traumatic spinal cord white matter injury. J. Neurotrauma **15,** 929–941.

BAMBER, N.I., LI, H., LU, X., et al. (2001). Neurotrophins BDNF and NT-3 promote axonal re-entry into the distal host spinal cord through Schwann cell–seeded mini-channels. Eur. J. Neurosci. **13,** 257–268.

BASSO, D.M., BEATTIE, M.S., and BRESNAHAN, J.C. (1995). A sensitive and reliable locomotor rating scale for open field testing in rats. J. Neurotrauma **12,** 1–21.

BLOCH, J., FINE, E.G., BOUCHE, N., et al. (2001). Nerve growth factor– and neurotrophin-3–releasing guidance channels promote regeneration of the transected rat dorsal root. Exp. Neurol. **172,** 425–432.

BRADBURY, E.J., MOON, L.D., POPAT, R.J., et al. (2002). Chondroitinase ABC promotes functional recovery after spinal cord injury. Nature **416,** 636–640.

BROOK, G.A., PLATE, D., FRANZEN, R., et al. (1998). Spontaneous longitudinally orientated axonal regeneration is associated with the Schwann cell framework within the lesion site following spinal cord compression injury of the rat. J. Neurosci. Res. **53,** 51–65.

BUNGE, M.B. (1994). Transplantation of purified populations of Schwann cells into lesioned adult rat spinal cord. J. Neurol. **242,** S36–S39.

CAMPBELL, J.B., BASSETT, C.A.L., HUSBY, J., et al. (1957). Regeneration of adult mammalian spinal cord. Science **126,** 929.

CHAMBERLAIN, L.J., YANNAS, I.V., HSU, H.P., et al. (1998). Collagen-GAG substrate enhances the quality of nerve regeneration through collagen tubes up to level of autograft. Exp. Neurol. **154,** 315–329.

CHANG, G.L., HUNG, T.K., and FENG, W.W. (1988). An *in-vivo* measurement and analysis of viscoelastic properties of the spinal cord of cats. J. Biomech. Eng. **110,** 115–122.

CHEN, A., XU, X.M., KLEITMAN, N., et al. (1996). Methylprednisolone administration improves axonal regeneration into Schwann cell grafts in transected adult rat thoracic spinal cord. Exp. Neurol. **138,** 261–276.

CHENG, H., CAO, Y., and OLSON, L. (1996). Spinal cord repair in adult paraplegic rats: partial restoration of hind limb function. Science **273,** 510–513.

CHOI, D., LI, D., and RAISMAN, G. (2002). Fluorescent retrograde neuronal tracers that label the rat facial nucleus: a comparison of Fast Blue, Fluoro-ruby, Fluoro-emerald, Fluoro-Gold and DiI. J. Neurosci. Methods **117,** 167–172.

COUMANS, J.V., LIN, T.T., DAI, H.N., et al. (2001). Axonal regeneration and functional recovery after complete spinal cord transection in rats by delayed treatment with transplants and neurotrophins. J. Neurosci. **21,** 9334–9344.

DAHLIN, L.B., and LUNDBORG, G. (2001). Use of tubes in peripheral nerve repair. Neurosurg. Clin. North Am. **12,** 341–352.

DALTON, P.D., FLYNN, L., and SHOICHET, M.S. (2002). Manufacture of poly(2-hydroxyethyl methacrylate-co-methyl methacrylate) hydrogel tubes for use as nerve guidance channels. Biomaterials **23,** 3843–3851.

DALTON, P.D., and SHOICHET, M.S. (2001). Creating porous tubes by centrifugal forces for soft tissue application. Biomaterials **22,** 2661–2669.

DOWSON, J.H., and HARRIS, S.J. (1981). Quantitative studies of the autofluorescence derived from neuronal lipofuscin. J. Microsc. **123,** 249–258.

FIELDS, R.D., LE BEAU, J.M., LONGO, F.M., et al. (1989). Nerve regeneration through artificial tubular implants. Prog. Neurobiol. **33,** 87–134.

FITCH, M.T., DOLLER, C., COMBS, C.K., et al. (1999). Cellular and molecular mechanisms of glial scarring and progressive cavitation: *in vivo* and *in vitro* analysis of inflammation-induced secondary injury after CNS trauma. J. Neurosci. **19,** 8182–8198.

FOUAD, K., DIETZ, V., and SCHWAB, M.E. (2001). Improving axonal growth and functional recovery after experimental spinal cord injury by neutralizing myelin associated inhibitors. Brain Res. Brain Res. Rev. **36,** 204–212.

FRIEDMAN, J.A., WINDEBANK, A.J., MOORE, M.J., et al. (2002). Biodegradable polymer grafts for surgical repair of the injured spinal cord. Neurosurgery **51,** 742–752.

GAUTIER, S.E., OUDEGA, M., FRAGOSO, M., et al. (1998). Poly(alpha-hydroxyacids) for application in the spinal cord: resorbability and biocompatibility with adult rat Schwann cells and spinal cord. J. Biomed. Mater. Res. **42,** 642–654.

GUENARD, V., KLEITMAN, N., MORRISSEY, T.K., et al. (1992). Syngeneic Schwann cells derived from adult nerves seeded in semipermeable guidance channels enhance peripheral nerve regeneration. J. Neurosci. **12,** 3310–3320.

GUEST, J.D., RAO, A., OLSON, L., et al. (1997). The ability of human Schwann cell grafts to promote regeneration in the transected nude rat spinal cord. Exp. Neurol. **148,** 502–522.

HIEBERT, G.W., KHODARAHMI, K., MCGRAW, J., et al. (2002). Brain-derived neurotrophic factor applied to the motor cortex promotes sprouting of corticospinal fibers but not regeneration into a peripheral nerve transplant. J. Neurosci. Res. **69,** 160–168.

HUANG, D.W., MCKERRACHER, L., BRAUN, P.E., et al. (1999). A therapeutic vaccine approach to stimulate axon regeneration in the adult mammalian spinal cord. Neuron **24,** 639–647.

HUNG, T.K., CHANG, G.L., LIN, H.S., et al. (1981). Stress-strain relationship of the spinal cord of anesthetized cats. J. Biomech. **14,** 269–276.

KWON, B.K., LIU, J., MESSERER, C., et al. (2002). Survival and regeneration of rubrospinal neurons 1 year after spinal cord injury. Proc. Natl. Acad. Sci. USA **99,** 3246–3251.

LEVINE, J.M., and NISHIYAMA, A. (1996). The NG2 chondroitin sulfate proteoglycan: a multifunctional proteoglycan associated with immature cells. Perspect. Dev. Neurobiol. **3,** 245–259.

LIU, Y., HIMES, B.T., MURRAY, M., et al. (2002). Grafts of BDNF-producing fibroblasts rescue axotomized rubrospinal neurons and prevent their atrophy. Exp. Neurol. **178,** 150–164.

LU, J., FERON, F., MACKAY-SIM, A., et al. (2002). Olfactory ensheathing cells promote locomotor recovery after delayed transplantation into transected spinal cord. Brain **125,** 14–21.

LUNDBORG, G., DAHLIN, L.B., DANIELSEN, N.P., et al. (1981). Reorganization and orientation of regenerating nerve fibres, perineurium, and epineurium in preformed mesothelial tubes—an experimental study on the sciatic nerve of rats. J. Neurosci. Res. **6,** 265–281.

LUO, Y., DALTON, P.D., and SHOICHET, M.S. (2001). Investigating the properties of novel poly(2-hydroxethyl methacrylate-co-methyl methacrylate) hydrogel hollow fiber membranes. Chem. Mater. **13,** 4087–4093.

MACKINNON, S.E., and DELLON, A.L. (1990). Clinical nerve reconstruction with a bioabsorbable polyglycolic acid tube. Plas. Reconstr. Surg. **85,** 419–424.

MCTIGUE, D.M., WEI, P., and STOKES, B.T. (2001). Proliferation of NG2-positive cells and altered oligodendrocyte numbers in the contused rat spinal cord. J. Neurosci. **21,** 3392–3400.

MEEK, M.F., DEN DUNNEN, W.F., SCHAKENRAAD, J.M., et al. (1996). Evaluation of functional nerve recovery after reconstruction with a poly (DL-lactide-epsilon-caprolactone) nerve guide, filled with modified denatured muscle tissue. Microsurgery **17,** 555–561.

MONTGOMERY, C.T., TENAGLIA, E.A., and ROBSON, J.A. (1996). Axonal growth into tubes implanted within lesions in the spinal cords of adult rats. Exp. Neurol. **137,** 277–290.

NAMIKI, J., KOJIMA, A., and TATOR, C.H. (2000). Effect of brain-derived neurotrophic factor, nerve growth factor, and neurotrophin-3 on functional recovery and regeneration after spinal cord injury in adult rats. J. Neurotrauma **17,** 1219–1231.

ONG, W.Y., and LEVINE, J.M. (1999). A light and electron microscopic study of NG2 chondroitin sulfate proteoglycan-positive oligodendrocyte precursor cells in the normal and kainate-lesioned rat hippocampus. Neuroscience **92,** 83–95.

OUDEGA, M., GAUTIER, S.E., CHAPON, P., et al. (2001). Axonal regeneration into Schwann cell grafts within resorbable poly(alpha-hydroxyacid) guidance channels in the adult rat spinal cord. Biomaterials **22,** 1125–1136.

OUDEGA, M., XU, X.M., GUENARD, V., et al. (1997). A combination of insulin-like growth factor–I and platelet-derived growth factor enhances myelination but diminishes ax-

onal regeneration into Schwann cell grafts in the adult rat spinal cord. Glia **19,** 247–258.

POPOVICH, P.G., WEI, P., and STOKES, B.T. (1997). Cellular inflammatory response after spinal cord injury in Sprague-Dawley and Lewis rats. J. Comp. Neurol. **377,** 443–464.

RAMON-CUETO, A., PLANT, G.W., AVILA, J., et al. (1998). Long-distance axonal regeneration in the transected adult rat spinal cord is promoted by olfactory ensheathing glia transplants. J. Neurosci. **18,** 3803–3815.

RAPALINO, O., LAZAROV-SPIEGLER, O., AGRANOV, E., et al. (1998). Implantation of stimulated homologous macrophages results in partial recovery of paraplegic rats. Nat. Med. **4,** 814–821.

RODRIGUEZ, F.J., GOMEZ, N., PEREGO, G., et al. (1999). Highly permeable polylactide-caprolactone nerve guides enhance peripheral nerve regeneration through long gaps. Biomaterials **20,** 1489–1500.

SALACINSKI, H.J., GOLDNER, S., GIUDICEANDREA, A., et al. (2001). The mechanical behavior of vascular grafts: a review. J. Biomater. Appl. **15,** 241–278.

SCHMUED, L.C., and FALLON, J.H. (1986). Fluoro-Gold: a new fluorescent retrograde axonal tracer with numerous unique properties. Brain Res. **377,** 147–154.

SCHNELL, L., SCHNEIDER, R., KOLBECK, R., et al. (1994). Neurotrophin-3 enhances sprouting of corticospinal tract during development and after adult spinal cord lesion. Nature **367,** 170–173.

SCHUMACHER, P.A., EUBANKS, J.H., and FEHLINGS, M.G. (1999). Increased calpain I–mediated proteolysis, and preferential loss of dephosphorylated NF200, following traumatic spinal cord injury. Neuroscience **91,** 733–744.

SCHWARTZ, M., LAZAROV-SPIEGLER, O., RAPALINO, O., et al. (1999). Potential repair of rat spinal cord injuries using stimulated homologous macrophages. Neurosurgery **44,** 1041–1046.

SPILKER, M.H., YANNAS, I.V., HSU, H.P., et al. (1997). The effects of collagen-based implants on early healing of the adult rat spinal cord. Tissue Eng. **3,** 309–317.

SPILKER, M.H., YANNAS, I.V., KOSTYK, S.K., et al. (2001). The effects of tubulation on healing and scar formation after transection of the adult rat spinal cord. Restor. Neurol. Neurosci. **18,** 23–38.

STOJANOVIC, A., ROHER, A.E., and BALL, M.J. (1994). Quantitative analysis of lipofuscin and neurofibrillary tangles in the hippocampal neurons of Alzheimer disease brains. Dementia **5,** 229–233.

TAYLOR, M., VERDONSCHOT, N., HUISKES, R., et al. (1999). A combined finite element method and continuum damage mechanics approach to simulate the *in vitro* fatigue behavior of human cortical bone. J. Mater. Sci. Mater. Med. **10,** 841–846.

TENG, Y.D., LAVIK, E.B., QU, X., et al. (2002). Functional recovery following traumatic spinal cord injury mediated by a unique polymer scaffold seeded with neural stem cells. Proc. Natl. Acad. Sci. USA **99,** 3024–3029.

TSAI, E.C., VAN BENDEGEM, R.L., HWANG, S.W., et al. (2001). A novel method for simultaneous anterograde and retrograde labeling of spinal cord motor tracts in the same animal. J. Histochem. Cytochem. **49,** 1111–1122.

TUSZYNSKI, M.H., WEIDNER, N., MCCORMACK, M., et al. (1998). Grafts of genetically modified Schwann cells to the spinal cord: survival, axon growth, and myelination. Cell Transplant. **7,** 187–196.

VERDU, E., NAVARRO, X., GUDINO-CABRERA, G., et al. (1999). Olfactory bulb ensheathing cells enhance peripheral nerve regeneration. Neuroreport **10,** 1097–1101.

WATANABE, M., TOYAMA, Y., and NISHIYAMA, A. (2002). Differentiation of proliferated NG2-positive glial progenitor cells in a remyelinating lesion. J. Neurosci. Res. **69,** 826–836.

WELLS, M.R., KRAUS, K., BATTER, D.K., et al. (1997). Gel matrix vehicles for growth factor application in nerve gap injuries repaired with tubes: a comparison of biomatrix, collagen, and methylcellulose. Exp. Neurol. **146,** 395–402.

WOERLY, S., DOAN, V.D., EVANS-MARTIN, F., et al. (2001). Spinal cord reconstruction using NeuroGel implants and functional recovery after chronic injury. J. Neurosci. Res. **66,** 1187–1197.

XU, X.M., CHEN, A., GUENARD, V., et al. (1997). Bridging Schwann cell transplants promote axonal regeneration from both the rostral and caudal stumps of transected adult rat spinal cord. J. Neurocytol. **26,** 1–16.

XU, X.M., GUENARD, V., KLEITMAN, N., et al. (1995). Axonal regeneration into Schwann cell–seeded guidance channels grafted into transected adult rat spinal cord. J. Comp. Neurol. **351,** 145–160.

XU, X.M., ZHANG, S.X., LI, H., et al. (1999). Regrowth of axons into the distal spinal cord through a Schwann-cell–seeded mini-channel implanted into hemisected adult rat spinal cord. Eur. J. Neurosci. **11,** 1723–1740.

ZUO, J., NEUBAUER, D., DYESS, K., et al. (1998). Degradation of chondroitin sulfate proteoglycan enhances the neurite-promoting potential of spinal cord tissue. Exp. Neurol. **154,** 654–662.

Address reprint requests to:
Charles H. Tator, M.D., Ph.D.
Division of Cellular and Molecular Biology
Toronto Western Research Institute
Toronto Western Hospital
Room 4W-433
399 Bathurst St.
Toronto, ON, Canada M5T 2S8

E-mail: charles.tator@uhn.on.ca.

EVE C. TSAI

AU1
City & state for Dynatek